HHS Public Access

Author manuscript

Cell. Author manuscript; available in PMC 2018 June 01.

Published in final edited form as:

Cell. 2017 June 01; 169(6): 1130–1141.e11. doi:10.1016/j.cell.2017.05.005.

Interferon-γ drives T_{reg} fragility to promote anti-tumor immunity

Abigail E Overacre-Delgoffe[1,2], **Maria Chikina**[3], **Rebekah E Dadey**[1], **Hiroshi Yano**[1], **Erin A Brunazzi**[1], **Gulidanna Shayan**[4], **William Horne**[5], **Jessica M Moskovitz**[4,8], **Jay K Kolls**[1,5], **Cindy Sander**[7], **Yongli Shuai**[6], **Daniel P Normolle**[6], **John M Kirkwood**[1,7], **Robert L Ferris**[1,4,8], **Greg M Delgoffe**[1,2,4], **Tullia C Bruno**[1,4], **Creg J Workman**[1,2], and **Dario AA Vignali**[1,2,4,9]

[1]Department of Immunology, University of Pittsburgh School of Medicine, Pittsburgh, PA 15213, USA

[2]Department of Immunology, St. Jude Children's Research Hospital, Memphis, TN 38105, USA

[3]Department of Computational and Systems Biology, University of Pittsburgh School of Medicine, Pittsburgh, PA 15261, USA

[4]Tumor Microenvironment Center, University of Pittsburgh Cancer Institute, Pittsburgh PA 15232, USA

[5]Richard King Mellon Foundation Institute for Pediatric Research, Children's Hospital of Pittsburgh of University of Pittsburgh Medical Center, Pittsburgh, PA 15224, USA

[6]UPCI Biostatistics Facility, University of Pittsburgh Medical Center, Pittsburgh, PA 15213, USA

[7]Division of Hematology-Oncology, Department of Medicine, University of Pittsburgh Medical Center, Pittsburgh, PA 15232, USA

[8]Department of Otolaryngology, University of Pittsburgh and University of Pittsburgh Cancer Institute, Pittsburgh PA 15213, USA

Summary

Regulatory T cells (T_{regs}) are a barrier to anti-tumor immunity. Neuropilin-1 (Nrp1) is required to maintain intratumoral T_{reg} stability and function but is dispensable for peripheral immune tolerance. T_{reg}-restricted Nrp1 deletion results in profound tumor resistance due to T_{reg} functional fragility. Thus, identifying the basis for Nrp1 dependency and the key drivers of T_{reg} fragility could help to improve immunotherapy for human cancer. We show that a high percentage of intratumoral $NRP1^+$ T_{regs} correlates with poor prognosis in melanoma and head and neck squamous cell carcinoma. Using a mouse model of melanoma where Nrp1-deficient ($Nrp1^{-/-}$) and

Correspondence to: Dario AA Vignali.

[9]Lead Contact.

Author Contributions: Conceptualization, A.E.O.D., and D.A.A.V.; Formal Analysis, M.C., D.P.N., Y.S.; Investigation, A.E.O.D., H.Y., R.E.D., E.A.B., G.S., W.H., G.M.D., T.C.B.; Resources, J.M.M., C.S., J.M.K., R.L.F.; Writing – Original Draft, A.E.O.D. and D.A.A.V.; Writing – Review & Editing, A.E.O.D., M.C., R.E.D., H.Y,. E.A.B., G.S., W.H., J.M.M., J.K.K., J.M.K., R.L.F., C.S., D.P.N., Y.S., G.M.D., T.C.B., C.J.W., D.A.A.V.; Supervision, J.K.K., T.C.B., C.J.W., D.A.A.V.

wild-type (*Nrp1*$^{+/+}$) T_{regs} can be assessed in a competitive environment, we find that a high proportion of intratumoral *Nrp1*$^{-/-}$ T_{regs} produce interferon-γ (IFNγ), which drives the fragility of surrounding WT T_{regs}, boosts anti-tumor immunity, and facilitates tumor clearance. We also show that IFNγ-induced T_{reg} fragility is required for response to anti-PD1, suggesting that cancer therapies promoting T_{reg} fragility may be efficacious.

Graphical abstract

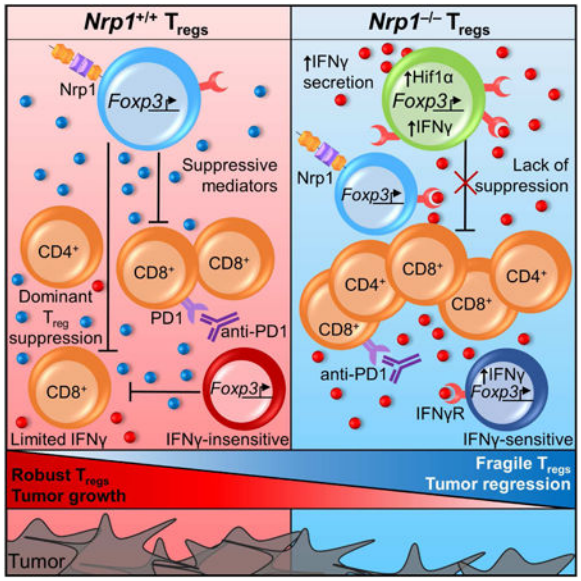

Introduction

Regulatory T cells (T_{regs}), characterized by their expression of the forkhead box transcription factor, *Foxp3*, are required to maintain immune homeostasis and prevent excessive tissue damage (Fontenot et al., 2005; Kim et al., 2007; Miyara and Sakaguchi, 2007; Vignali et al., 2008). Humans that lack a functional T_{reg} population develop a lethal autoimmune disorder, termed Immune dysregulation, Polyendocrinopathy, Enteropathy, X-linked (IPEX) syndrome, which can be recapitulated in mice through *Foxp3* deletion. While T_{regs} are required to limit autoimmunity and maintain immune regulation, they can be deleterious in cancer through suppression of anti-tumor immunity (Chaudhry and Rudensky, 2013; Facciabene et al., 2012; Liu et al., 2016). Indeed, high numbers of T_{regs} and a low $CD8^+$ T cell:T_{reg} ratio are considered poor prognostic factors for many tumor types, including melanoma, head and neck squamous cell carcinoma (HNSCC), ovarian cancer and colorectal carcinoma (Curiel et al., 2004; Drennan et al., 2013; Jacobs et al., 2012; Nishikawa and Sakaguchi, 2010; Saito et al., 2016). Although targeting intratumoral T_{regs} could be an effective therapeutic approach for multiple tumor types, perturbation of peripheral T_{reg} number or function could lead to life-threatening autoimmune or inflammatory complications. Therefore, identifying pathways that could be targeted to selectively undermine intratumoral T_{regs} is essential.

We have previously shown that Neuropilin-1 (Nrp1) is expressed by ~90% of tumor infiltrating T_{regs} in mouse models of cancer and is critical for their function in the tumor microenvironment (Delgoffe et al., 2013). Indeed, mice with a T_{reg}-restricted deletion of Nrp1 are highly resistant to B16 melanoma, which is normally refractory to immune-mediated clearance, yet remarkably do not exhibit any autoimmune or inflammatory disease. Although we have previously described Nrp1-deficient T_{regs} as 'unstable', due to their loss of function (Delgoffe et al., 2013), previous studies and data included here clearly show that they retain Foxp3 expression. Thus, we now refer to this phenotype as T_{reg} 'fragility' consistent with their retention of Foxp3 expression yet loss of function *ex vivo* (as exhibited by loss of suppressive activity *in vitro*) and tumor tolerance *in vivo* (as exhibited by tumor growth reduction/clearance). While our previous data demonstrated the importance of Nrp1 in maintaining intratumoral T_{reg} function, many questions remain including the fate of these fragile T_{regs} and their contribution to anti-tumor immunity, the drivers of T_{reg} fragility, the expression, contribution, and impact of NRP1 on human intratumoral T_{regs}, and the broader implications for T_{reg} function and cancer immunotherapy.

Results

Increased NRP1 expression on T_{regs} in human cancer

While Nrp1 has been shown to prevent T_{reg} fragility in mice, its presence and role in human T_{regs} remains unclear. Previous studies have been controversial, with some suggesting peripheral human T_{regs} do not express NRP1 while other suggest that $NRP1^+$ T_{regs} are potent suppressors (Battaglia et al., 2009; Battaglia et al., 2008; Chaudhary and Elkord, 2015; Chaudhary et al., 2014; Gao et al., 2016; Milpied et al., 2009; Piechnik et al., 2013; Tatura et al., 2015). Indeed, very few human T_{regs} in peripheral blood lymphocytes (PBL) from healthy donors express NRP1 (Fig. 1A and B). Remarkably, most patients with metastatic melanoma and head and neck squamous cell carcinoma (HNSCC) possessed a reasonably high percentage of intratumoral $NRP1^+$ T_{regs} (Fig. 1A and B). This varied considerably from 3-90% in melanoma and 35-90% in HNSCC. The percentage of $NRP1^+$ T_{regs} in PBL was also substantially enhanced. Interestingly, NRP1 expression in intratumoral T_{regs} appeared to correlated with poor prognosis in both melanoma and HNSCC (Fig. 1C).

Nrp1$^{-/-}$ T_{regs} block wild type T_{reg} function and promote anti-tumor immunity

We have previously shown that anti-Nrp1 substantially limits the growth of a B16 mouse model of human melanoma (Delgoffe et al., 2013). Given the heterogeneous nature of NRP1 expression on human tumor infiltrating T_{regs}, where only a proportion express NRP1, we questioned what impact Nrp1 loss on only a proportion of mouse T_{regs} might have on the function of the remaining wild-type (WT) counterparts, and by extension anti-tumor immunity and tumor growth. Also, as *Nrp1*-deficient T_{regs} show a reduction in suppressive function but also an increase in effector phenotype (Delgoffe et al., 2013), we questioned whether these cells had an active role in re-shaping the tumor microenvironment, or whether reduced tumor growth was instead due to reduction of a major suppressive cell population.

Foxp3 is on the X chromosome and is thus subject to X inactivation (Briggs and Reijo Pera, 2014; Galupa and Heard, 2015; Lee and Bartolomei, 2013), rendering only one allele active in each T_{reg}. Consequently in heterozygous *Nrp1*$^{L/L}$*Foxp3*$^{Cre\text{-}YFP/DTR\text{-}GFP}$ female mice, 50% of T_{regs} have a Cre-mediated deletion of *Nrp1*, are marked with YFP [herein referred to as *Nrp1*$^{-/-}$ T_{regs}] and exhibit functional fragility, and the other 50% express DTR-GFP and are WT T_{regs}, as they carry the *Nrp1*$^{L/L}$ allele but not *Foxp3*$^{Cre\text{-}YFP}$ [herein referred to as *Nrp1*$^{+/+}$ T_{regs}] (Fig. 1D). We first assessed tumor growth in heterozygous *Nrp1*$^{L/L}$Foxp3$^{Cre\text{-}YFP/DTR\text{-}GFP}$ female mice, with *Nrp1*$^{L/L}$*Foxp3*$^{Cre\text{-}YFP/Cre\text{-}YFP}$ [all T_{regs} are *Nrp1*$^{-/-}$] and *Foxp3*$^{Cre\text{-}YFP/Cre\text{-}YFP}$ [all T_{regs} are WT/*Nrp1*$^{+/+}$] female mice as controls. Strikingly, *Nrp1*$^{L/L}$*Foxp3*$^{Cre\text{-}YFP/DTR\text{-}GFP}$ mice exhibited dramatically reduced tumor growth, enhanced survival, and increased intratumoral lymphocyte and $CD8^+$ T cell number, phenocopying *Nrp1*$^{L/L}$*Foxp3*$^{Cre\text{-}YFP/Cre\text{-}YFP}$ mice (Fig. 1E and fig. S1A) (Delgoffe et al., 2013). This occurred despite the presence of *Nrp1*$^{+/+}$ T_{regs} in similar numbers to *Nrp1*$^{-/-}$ T_{regs} in the tumor (fig. S1A). A previous study had suggested that the absence of Nrp1 leads to reduced influx of T_{regs} into certain tumor types (Hansen et al., 2012). However, there did not seem to be a significant difference in the number of intratumoral *Nrp1*$^{-/-}$ versus *Nrp1*$^{+/+}$ T_{regs}, even in *Nrp1*$^{L/L}$*Foxp3*$^{Cre\text{-}YFP/DTR\text{-}GFP}$ mice (fig. S1A). One might also argue that the *Nrp1*$^{L/L}$*Foxp3*$^{Cre\text{-}YFP}$ mutation causes a basal inflammatory state that impacts the establishment of a tumor mass. To rule this out and any potential impact Nrp1 loss may have on T_{reg} development, migration and function, the impact of *Nrp1* temporal deletion in T_{regs} following the establishment of B16 tumor growth was determined. *Nrp1*$^{L/L}$*Foxp3*^{CreERT2}, but not *Foxp3*^{CreERT2}, mice exhibited substantially reduced tumor growth following *Nrp1* deletion induced by daily tamoxifen treatment on Days 7-11 (fig. S1B-C).

To rule out the possibility that the inability of *Nrp1*$^{+/+}$ T_{regs} to block anti-tumor immunity and tumor clearance was due to their reduced number in heterozygous *Nrp1*$^{L/L}$*Foxp3*$^{Cre\text{-}YFP/DTR\text{-}GFP}$ mice, we also assessed tumor growth in heterozygous *Foxp3*$^{DTR\text{-}GFP/+}$ female mice in which diphtheria toxin (DT) treatment reduced peripheral and intratumoral T_{reg} number by approximately half (Fig. 1F and fig. S1D). In stark contrast to tumor growth in heterozygous *Nrp1*$^{L/L}$*Foxp3*$^{Cre\text{-}YFP/DTR\text{-}GFP}$ mice, DT-treated heterozygous *Foxp3*$^{DTR\text{-}GFP/+}$ mice exhibited tumor growth that was indistinguishable from the untreated control mice (Fig. 1G). While *Foxp3*$^{DTR\text{-}GFP/DTR\text{-}GFP}$ mice treated with DT largely cleared their tumors, they ultimately succumbed to autoimmunity due to an absence of T_{regs} in contrast to heterozygous *Nrp1*$^{L/L}$*Foxp3*$^{Cre\text{-}YFP/DTR\text{-}GFP}$ and *Nrp1*$^{L/L}$*Foxp3*$^{Cre\text{-}YFP/Cre\text{-}YFP}$ female mice that never exhibited an autoimmune or inflammatory phenotype (Fig. 1D and 1E, and data not shown) (Delgoffe et al., 2013). Taken together, our data suggest that if half the T_{regs} are depleted tumors grow unrestrained, as the reduced number of WT T_{regs} are still capable of blocking anti-tumor immunity. In contrast, if half the T_{regs} lose *Nrp1*, tumors are controlled, suggesting that *Nrp1*$^{-/-}$ T_{regs} are playing an active role in re-shaping the tumor microenvironment.

It is possible that *Nrp1*$^{-/-}$ T_{regs} impact the tumor microenvironment by losing *Foxp3* and becoming so-called ex-T_{regs} with an altered functional phenotype (Overacre and Vignali, 2016; Zhou et al., 2009b). Indeed, we have previously shown that Nrp1 contributes to T_{reg} stability in the tumor microenvironment by undermining the pAKT:FOXO pathway and preventing the expression of T helper lineage-defining transcription factors, raising the

possibility that this may also result in the loss of *Foxp3* expression. We analyzed *Foxp3* fate mapping mice in which T_{regs} either possessed (*Foxp3*$^{Cre\text{-}YFP}$*Rosa*$^{L\text{-}Tom\text{-}L\text{-}GFP}$) or lacked *Nrp1* expression (*Nrp1*$^{L/L}$*Foxp3*$^{Cre\text{-}YFP}$*Rosa*$^{L\text{-}Tom\text{-}L\text{-}GFP}$) (fig. S2A). In this mouse model, non-T_{regs} are Tomato^{+}GFP^{-}YFP^{-}, *Foxp3*$^{+}$ T_{regs} are Tomato^{-}GFP^{+}YFP^{+} and *Foxp3*$^{-}$ ex-T_{regs} are Tomato^{-}GFP^{+}YFP^{-}. Interestingly, there were very few (<5%) ex-T_{regs} present in the periphery or in the tumor, regardless of Nrp1 expression (fig. S2B and C). These data suggest that the absence of Nrp1 does not affect *Foxp3* expression and does not result in the generation of ex-T_{regs}.

Previous reports have shown that T_{regs} can display alternative functions *in vivo* while maintaining *Foxp3* expression (Hori, 2014; Sharma et al., 2013). We hypothesized that *Nrp1*$^{-/-}$ T_{regs} not only lost their suppressive activity but may also negatively impact the function of surrounding intratumoral *Nrp1*$^{+/+}$ T_{regs}. In order to assess this possibility, we determined the suppressive capacity of *Nrp1*$^{+/+}$ (GFP^{+}) and *Nrp1*$^{-/-}$ (YFP^{+}) T_{regs} from *Nrp1*$^{L/L}$*Foxp3*$^{Cre\text{-}YFP/DTR\text{-}GFP}$ heterozygous and control mice using a microsuppression assay (Turnis et al., 2016). While all T_{reg} populations isolated from non-draining lymph nodes (ndLN) were equally capable of suppressing effector T cells (Fig. 1H), *Nrp1*$^{-/-}$ T_{regs} isolated from homozygous *Nrp1*$^{L/L}$*Foxp3*$^{Cre\text{-}YFP/Cre\text{-}YFP}$ and heterozygous *Nrp1*$^{L/L}$*Foxp3*$^{Cre\text{-}YFP/DTR\text{-}GFP}$ tumors lacked suppressive activity (Fig. 1H). Interestingly, intratumoral *Nrp1*$^{+/+}$ T_{regs} isolated from heterozygous *Nrp1*$^{L/L}$*Foxp3*$^{Cre\text{-}YFP/DTR\text{-}GFP}$ mice were also unable to suppress. Two hallmarks of T_{reg} fragility are elevated pAkt and reduced ICOS expression (Delgoffe et al., 2013). Elevated pAkt and reduced ICOS were observed in *Nrp1*$^{-/-}$ T_{regs} in *Nrp1*$^{L/L}$*Foxp3*$^{Cre\text{-}YFP/Cre\text{-}YFP}$ mice and *Nrp1*$^{L/L}$*Foxp3*$^{Cre\text{-}YFP/DTR\text{-}GFP}$ heterozygous mice relative to *Nrp1*$^{+/+}$ T_{regs} in *Foxp3*$^{Cre\text{-}YFP/Cre\text{-}YFP}$ mice as expected (fig. S2D and E). However, elevated pAkt and, to a lesser extent, reduced ICOS was also observed in *Nrp1*$^{+/+}$ T_{regs} in *Nrp1*$^{L/L}$*Foxp3*$^{Cre\text{-}YFP/DTR\text{-}GFP}$ heterozygous mice. Taken together, these data suggest that *Nrp1*$^{-/-}$ T_{regs} have a negative impact on the suppressive function of intratumoral *Nrp1*$^{+/+}$ T_{regs}.

Fragile and wild type T_{regs} have a reciprocal impact on their transcriptome

We next used transcriptomic analysis of *Nrp1*$^{+/+}$ and *Nrp1*$^{-/-}$ T_{regs} from *Foxp3*$^{Cre\text{-}YFP/Cre\text{-}YFP}$, *Nrp1*$^{L/L}$*Foxp3*$^{Cre\text{-}YFP/Cre\text{-}YFP}$ and *Nrp1*$^{L/L}$*Foxp3*$^{Cre\text{-}YFP/DTR\text{-}GFP}$ mice to evaluate the cell intrinsic and extrinsic impact of *Nrp1* loss (fig. S3). Significant alterations in the T_{reg} transcriptome were observed between *Nrp1*$^{+/+}$ and *Nrp1*$^{-/-}$ T_{regs}. Principal Component Analysis (PCA) based on differentially expressed genes clearly separated T_{eff} and T_{regs} based on both location and genotype. Interestingly, intratumoral *Nrp1*$^{+/+}$ and *Nrp1*$^{-/-}$ T_{regs} from heterozygous *Nrp1*$^{L/L}$*Foxp3*$^{Cre\text{-}YFP/DTR\text{-}GFP}$ mice were similar to each other and yet distinct from their genotypically identical counterparts from control *Foxp3*$^{Cre\text{-}YFP/Cre\text{-}YFP}$ and *Nrp1*$^{L/L}$*Foxp3*$^{Cre\text{-}YFP/Cre\text{-}YFP}$ mice (Fig. 2A, fig. S4A-B). A similar impact was observed when T_{reg} signature genes were assessed wherein it became evident that all four populations were district and yet bore a transcriptional relationship (fig. S4C). These data suggest that *Nrp1*$^{+/+}$ and *Nrp1*$^{-/-}$ T_{regs} in heterozygous *Nrp1*$^{L/L}$*Foxp3*$^{Cre\text{-}YFP/DTR\text{-}GFP}$ mice impact each other's transcriptome in a reciprocal manner.

Pathway analysis highlighted a potential role for IFNγ/IL-12-related transcriptional programs. Of particular interest was an increase in *Ifng* and its targets in *Nrp1*$^{-/-}$ T_{regs} in *Nrp1*$^{L/L}$*Foxp3*$^{Cre\text{-}YFP/Cre\text{-}YFP}$ and *Nrp1*$^{L/L}$*Foxp3*$^{Cre\text{-}YFP/DTR\text{-}GFP}$ as well as in *Nrp1*$^{+/+}$ T_{regs} in *Nrp1*$^{L/L}$*Foxp3*$^{Cre\text{-}YFP/DTR\text{-}GFP}$ mice (Fig. 2B-C, fig. S4D), implicating a role for the IFNγ pathway in modulating T_{reg} function and function in the tumor microenvironment.

While previous reports have suggested that a small subset of T_{regs} produce IFNγ during inflammation (Duhen et al., 2012; Koenecke et al., 2012; Pandiyan and Zhu, 2015), the expression of IFNγ by T_{regs} in tumors and its impact on their suppressive function remains unclear. Using flow cytometry, we found that there was increased expression of IFNγ by *Nrp1*$^{-/-}$ T_{regs} in both *Nrp1*$^{L/L}$*Foxp3*$^{Cre\text{-}YFP/Cre\text{-}YFP}$ and *Nrp1*$^{L/L}$*Foxp3*$^{Cre\text{-}YFP/DTR\text{-}GFP}$ mice (Fig. 3A-B). Interestingly, an increased percentage of *Nrp1*$^{+/+}$ T_{regs} from *Nrp1*$^{L/L}$*Foxp3*$^{Cre\text{-}YFP/DTR\text{-}GFP}$ mice also expressed IFNγ. Interferon-γ receptor 1 (IFNγR) expression showed an elevated trend in *Nrp1*$^{-/-}$ T_{regs} in *Nrp1*$^{L/L}$*Foxp3*$^{Cre\text{-}YFP/Cre\text{-}YFP}$ mice, and both *Nrp1*$^{-/-}$ and *Nrp1*$^{+/+}$ T_{regs} in *Nrp1*$^{L/L}$*Foxp3*$^{Cre\text{-}YFP/DTR\text{-}GFP}$ heterozygous mice (Fig. 3B). In addition, several type 1 helper T cell markers were upregulated in *Nrp1*$^{-/-}$ T_{regs}, such as Tbet, Cxcr3, and Eomes (fig. S5A–F) as well as downstream pSTAT1 in *Nrp1*$^{-/-}$ T_{regs} from *Nrp1*$^{L/L}$*Foxp3*$^{Cre\text{-}YFP/DTR\text{-}GFP}$ mice and pSTAT4 in all *Nrp1*$^{-/-}$ T_{regs} (fig. S5G, H).

In order to determine whether modulation of IFNγ and IFNγR expression also occurred following blockade of the Nrp1:Sema4a axis, we treated B16 tumor-bearing mice with Sema4aIg (Delgoffe et al., 2013). Indeed, Sema4aIg treatment decreased tumor size, and led to an unstable T_{reg} phenotype as assessed by increased IFNγ production and higher IFNγR expression (Fig. 3C-E). Surprisingly, we found that the majority of the IFNγ^{+} cells in the TIL of *Nrp1*$^{L/L}$*Foxp3*$^{Cre\text{-}YFP}$ and *Nrp1*$^{L/L}$*Foxp3*$^{Cre\text{-}YFP/DTR\text{-}GFP}$ were T_{regs} (Fig. 4A) and that the total percentage of IFNγ^{+} cells in TIL was small in the absence of T_{reg}-restricted Nrp1 deletion (Fig. 4B), raising the possibility that IFNγ production may be a dominant feature of T_{reg} fragility and thus could be affecting surrounding cells in the tumor microenvironment including *Nrp1*$^{+/+}$ T_{regs}.

While our data show that T_{regs} were the predominant source of intratumoral IFNγ in *Nrp1*$^{L/L}$*Foxp3*$^{Cre\text{-}YFP}$ and *Nrp1*$^{L/L}$*Foxp3*$^{Cre\text{-}YFP/DTR\text{-}GFP}$ mice, we could not rule out the possibility that IFNγ production by fragile T_{regs} was initially triggered, or potentiated by, the altered tumor microenvironment. Indeed, tumor size is greatly reduced and lymphocyte infiltration increased in *Nrp1*$^{L/L}$*Foxp3*$^{Cre\text{-}YFP}$ and *Nrp1*$^{L/L}$*Foxp3*$^{Cre\text{-}YFP/DTR\text{-}GFP}$ mice (Fig. 1E and fig. S1A). In order to address this possibility, we blocked the anti-tumor immune response and prevented tumor shrinkage by depleting CD8^{+} T cells (using anti-CD8) in B16 tumor bearing mice, and assessed T_{reg} phenotype and function. We found that CD8^{+} T cell depletion had no effect on the suppressive capacity in *Nrp1*$^{L/L}$*Foxp3*$^{Cre\text{-}YFP}$ and *Nrp1*$^{L/L}$*Foxp3*$^{Cre\text{-}YFP/DTR\text{-}GFP}$ mice. Indeed, *Nrp1*$^{-/-}$ T_{regs} exhibited increased IFNγ and Tbet protein expression along with reduced in suppressive capacity in an *in vitro* suppression assay, suggesting that T_{reg} fragility due to *Nrp1* loss is primarily due to a cell intrinsic mechanism rather than an extrinsic environmental effect due to increased CD8^{+} T cell infiltration, the ensuing anti-tumor response, and tumor size (Fig. 4C-E and fig. S5I).

However, a role for $CD8^+$ T cell-derived IFNγ in promoting T_{reg} fragility in this system cannot be ruled out.

Although cell-intrinsic processes downstream of *Nrp1* loss appeared to drive T_{reg} fragility, it is still possible that cell-extrinsic, environmental factors facilitated intratumoral T_{reg} fragility. Further analysis of our RNAseq data highlighted enhanced expression of *Hif1a* (hypoxia-inducible factor 1 alpha) in $Nrp1^{-/-}$ compared to $Nrp1^{+/+}$ intratumoral T_{regs} (Fig. 4F). Indeed, the percentage of $Hif1\alpha^+$ $Nrp1^{-/-}$ intratumoral T_{regs} and Hif1α protein expression within those T_{regs} was higher than their $Nrp1^{+/+}$ counterparts (Fig. 4G). Interestingly, Hif1α has been shown to be upregulated by Akt signaling which in turn led to increased IFN-γ production by T_{regs} (Dang et al., 2011; Lee et al., 2015). As Hif1α is upregulated in hypoxic conditions, we wondered whether hypoxia was capable of inducing T_{reg} fragility, analogous to the environment in which intratumoral T_{regs} reside. Remarkably, LN-derived T_{regs} from a naïve mouse showed increased IFN-γ and Tbet expression, and an elevated trend in Hif1α expression while retaining Foxp3 expression after being cultured for 3 days in hypoxic versus normoxic conditions (Fig. 4H and fig. S5J and K). These data suggest that the hypoxia:Hif1α axis may prime T_{regs} to become functionally fragile in the tumor microenvironment.

IFNγ is required and sufficient to drive intratumoral T_{reg} fragility

In order to test whether $Nrp1^{-/-}$ T_{regs} could directly impact the function of $Nrp1^{+/+}$ T_{regs}, and if this was mediated by IFNγ, we co-cultured ndLN- or tumor-derived $Nrp1^{+/+}$ T_{regs} from either Thy1.1 $Foxp3^{Cre\text{-}YFP}$ or $Ifngr1^{-/-}Foxp3^{Cre\text{-}YFP}$ mice (T_{regs} which lack the IFNγ receptor) with $Nrp1^{-/-}$ T_{regs} from Thy1.2 $Nrp1^{L/L}Foxp3^{Cre\text{-}YFP}$ mice prior to assessing their regulatory activity in a microsuppression assay (Fig. 5A). All cell populations were also cultured alone under the same conditions as controls, and as expected, T_{reg} populations cultured alone exhibited the expected suppressive capacity (Fig. 1H compared with Fig. 5B, left side columns). Note that APCs were not included in the 72h pre-culture prior to the T_{reg} microsuppression assay. Interestingly, TIL-derived $Nrp1^{+/+}$ T_{regs} that were co-cultured with tumor-derived $Nrp1^{-/-}$ T_{regs} lost their ability to suppress effector T cells, in contrast to ndLN-derived T_{regs} (Fig. 5B, right side columns). Loss of suppressive activity did not require cell-cell contact, but was dependent on IFNγR expression (Fig. 5B-D). In order to confirm that IFNγ was the sole cytokine responsible for $Nrp1^{+/+}$ T_{reg} fragility following co-culture with $Nrp1^{-/-}$ T_{regs}, we co-cultured $Nrp1^{+/+}$ and $Nrp1^{-/-}$ T_{regs} in the presence of different concentrations of anti-IFNγ for 72 hours, and then assessed the suppressive capacity of the purified $Nrp1^{+/+}$ T_{regs} in the absence of anti-IFNγ. IFNγ neutralization prevented the loss of tumor-derived $Nrp1^{+/+}$ T_{reg} suppression in a dose-dependent manner (Fig. 5E and fig. S6A). The increased sensitivity of tumor- versus ndLN-derived $Nrp1^{+/+}$ T_{regs} to $Nrp1^{-/-}$ T_{regs} appeared to correlate with IFNγR expression (fig. S6B).

While previous studies have suggested that IL-12 can impact T_{reg} suppression and induce IFNγ expression (Koch et al., 2012; Zhao et al., 2012), whether IFNγ has a direct effect on T_{regs} and if so what impact that might have in their function remains obscure. In order to determine whether IFNγ was sufficient to limit suppressive capacity, we treated $Nrp1^{+/+}$ T_{regs} from ndLN and TIL with IFNγ for 72 hours plus IL-2 in stimulating conditions prior

to assessing their functional capacity in a microsuppression assay in the absence of cytokine. IFNγ substantially limited the suppressive capacity of TIL-derived, and to a lesser extent ndLN-derived, *Nrp1*$^{+/+}$ T_{regs} in a dose-dependent manner (Fig. 5F). This effect was lost if *Ifngr1*$^{-/-}$ T_{regs} were used (fig. S6C). Pre-treatment with IFNγ also induced IFNγ expression by WT T_{regs} but not *Ifngr1*$^{-/-}$ T_{regs} (fig. S6D, and data not shown). Given that IFNγ limits the function of murine T_{regs}, we asked whether IFNγ could also impact human T_{regs} and whether this was enhanced by the human tumor microenvironment. Indeed, intratumoral human T_{regs} showed an increased sensitivity to IFNγ in comparison to PBL T_{regs} when cultured with the cytokine 72 hours prior to assessment of their suppressive capacity in the absence of cytokine (Fig. 5G). Furthermore, intratumoral NRP1^{+} T_{regs} appeared to be less sensitive to the effects of IFNγ than NRP1^{-} T_{regs}. Taken together, these data suggest that IFNγ can undermine the function of murine and human T_{regs} *in vitro*.

We next sought to determine if *Nrp1*$^{-/-}$ T_{reg}-derived IFNγ from could drive *Nrp1*$^{+/+}$ T_{reg} fragility *in vivo*. To address this, we used *Foxp3*$^{-/-}$ mice that lack T_{regs} and succumb to a scurfy-like phenotype if T_{regs} are not adoptively transferred within 48 hours of birth (Workman et al., 2011). T_{regs} of a single genotype or a 50:50 mixture of two different T_{reg} genotypes were adoptively transferred into two-day-old *Foxp3*$^{-/-}$ mice. At 4 weeks of age, mice were injected with B16 melanoma and tumor growth assessed over time (Fig. 6A). Mice were monitored after T_{reg} injection and removed from study prior to B16 injection if any signs of autoimmunity were observed (Workman et al., 2011). Tumor growth in *Foxp3*$^{-/-}$ mice that received either *Nrp1*$^{+/+}$ T_{regs}, *Nrp1*$^{-/-}$ T_{regs} or a 50:50 mixture of *Nrp1*$^{+/+}$ and *Nrp1*$^{-/-}$ T_{regs} phenocopied tumor growth in *Foxp3*$^{\text{Cre-YFP/Cre-YFP}}$, *Nrp1*$^{L/L}$*Foxp3*$^{\text{Cre-YFP/Cre-YFP}}$ and *Nrp1*$^{L/L}$*Foxp3*$^{\text{Cre-YFP/DTR-GFP}}$ mice, respectively (Fig. 1E and 6B-D and fig. S6E). We then assessed the impact of T_{reg}-derived IFNγ on tumor growth by transferring either [a] *Nrp1*$^{+/+}$ T_{regs} that cannot respond to IFNγ with *Nrp1*$^{-/-}$ T_{regs} (50% *Nrp1*$^{+/+}$*Ifngr1*$^{-/-}$ + 50% *Nrp1*$^{-/-}$*Ifngr1*$^{+/+}$), or [b] *Nrp1*$^{-/-}$ T_{regs} that cannot produce IFNγ with *Nrp1*$^{+/+}$ T_{regs} (50% *Nrp1*$^{+/+}$*Ifng*$^{+/+}$ + 50% *Nrp1*$^{-/-}$*Ifng*$^{-/-}$). Strikingly, tumor growth was completely restored with either combination (Fig. 6E-H), revealing a critical role for IFNγ produced by fragile *Nrp1*$^{-/-}$ T_{regs} in mediating *Nrp1*$^{+/+}$ T_{reg} dysfunction, and thereby facilitating anti-tumor immunity and limiting tumor growth.

IFN-γ-induced T_{reg} fragility is required for effective PD1-targeted immunotherapy

While our previous data suggested a prominent role for IFN-γ in driving T_{reg} fragility, the importance for this observation in the broader context of an immunotherapeutic response is unknown. We sought to address this question using mice that lack IFN-γR on T_{regs} (*Ifngr1*$^{L/L}$*Foxp3*$^{\text{Cre-YFP}}$) (fig. S7A and B). *Ifngr1*$^{L/L}$*Foxp3*$^{\text{Cre-YFP}}$ or *Foxp3*$^{\text{Cre-YFP}}$ mice were injected with 5×10^5 MC38 (an anti-PD1 sensitive tumor cell line) subcutaneously (SC) and then treated with either anti-PD1 or Armenian Hamster IgG control (200ug) on Days 6, 9 and 12 post-tumor injection. Strikingly, *Ifngr1*$^{L/L}$*Foxp3*$^{\text{Cre-YFP}}$ mice were completely resistant to PD1 blockade in comparison to *Foxp3*$^{\text{Cre-YFP}}$ mice, as exhibited by tumor growth and survival (Fig. 7A and fig. S7C). Consistent with the loss of IFN-γR expression preventing the development of T_{reg} fragility, no increase in percentage of IFNγ^{+} T_{regs} was observed in *Ifngr1*$^{L/L}$*Foxp3*$^{\text{Cre-YFP}}$ mice in contrast to *Foxp3*$^{\text{Cre-YFP}}$ mice following anti-

PD1 treatment (Fig. 7B). Taken together, these data suggest that IFN-γ-induced T_{reg} fragility is required for an effective response to PD1-targeted immunotherapy.

Discussion

In summary, our data highlight seven key observations. [i] A high proportion of human T_{regs} expressed NRP1 in two tumor types: melanoma and HNSCC. It is also noteworthy that PBL T_{regs} from these cancer patients also possessed a clear population of $NRP1^+$ T_{regs} in contrast to healthy donor PBL T_{regs}, which exhibited little to no NRP1 expression. Interestingly, the percentage of intratumoral $NRP1^+$ T_{regs} appeared to correlate with poor disease prognosis. [ii] B16 tumors were rapidly cleared in mice harboring a 50:50 mixture of Nrp1-deficient and WT T_{regs} due to increased functional fragility and loss of suppressive activity of both T_{reg} populations without loss of *Foxp3* expression. This was the result of Nrp1-deficient T_{reg} fragility rather than the generation of $Foxp3^-$ ex-T_{regs}. [iii] T_{reg} fragility had a reciprocal impact on the transcriptomes of Nrp1-deficient and WT T_{regs}, highlighting the previously unappreciated fact that T_{regs} can impact other T_{reg} populations directly as well as many other cell types. [iv] The induction of IFNγ pathway genes was a dominant feature of T_{reg} fragility in tumors. Intratumoral T_{regs} were more susceptible to this functionally fragile phenotype due to the hypoxic tumor microenvironment, which led to increased Hif1α expression and IFNγ production (Lee et al., 2015). While it is possible that IFNγ derived from other sources could lead to T_{reg} fragility, we have shown that hypoxia promoted IFNγ production and T_{reg} fragility. [v] IFNγ, exogenously-provided (human or mouse) or intratumoral *Nrp1*$^{-/-}$ T_{reg}-derived (mouse), was capable of driving the fragility of tumor-derived WT T_{regs} and loss of mouse and human T_{reg} suppressive activity *in vitro*. This was a direct effect of IFNγ or *Nrp1*$^{-/-}$ T_{reg}-derived IFNγ as no other cells types were included in the *in vitro* experiments. Previous studies have suggested that IL12 can impact T_{reg} suppression and induce IFNγ expression (Dominguez-Villar et al., 2011; Koch et al., 2012; Zhao et al., 2012), while others show that IFNγ can limit T_{reg} expansion (Deligne et al., 2015; Olalekan et al., 2015; St Rose et al., 2013; Visperas et al., 2014). However, the direct effect of IFNγ on T_{reg} function *in vivo* had surprisingly not been appreciated. While some studies have shown that $IFN\gamma^+$ T_{regs} can maintain suppressive function, this seems to be largely disease specific and has not been carefully assessed in the context of the tumor microenvironment (Oldenhove et al., 2009; Zhao et al., 2011). It is possible that the tumor microenvironment plays a critical role in driving IFNγ-mediated T_{reg} fragility, as suggested by the role of Hif1α in this process. In addition, while we anticipate that IL-12 may be playing a role in this process given that we see increased pSTAT4 expression, we have shown that IFNγ is capable of driving T_{reg} fragility both *in vitro* and *in vivo* in tumor-derived T_{regs} exposed to a hypoxic environment. (Figs. 5E-F and 6), suggesting that IL-12 may not be essential. [vi] Intratumoral T_{reg} fragility was mediated by IFNγ derived from *Nrp1*$^{-/-}$ T_{regs} that acted on WT intratumoral T_{regs}, thereby leading to their fragility and loss of suppressive activity. This was supported by the fact that inclusion of WT T_{regs} that could not respond to IFNγ or *Nrp1*$^{-/-}$ T_{regs} that could not produce IFNγ restored T_{reg} function, block anti-tumor immunity, and promote tumor growth. While these data suggest that *Nrp1*$^{-/-}$ T_{reg}-derived IFNγ is required, we do not yet know if it is sufficient. These observations were consistent with a model in which fragile *Nrp1*$^{-/-}$ T_{regs} produce large

amounts of IFNγ in the tumor microenvironment that directly promotes the fragility of intratumoral WT T_{regs} without loss of Foxp3 expression. Importantly, this occurred without any detectable peripheral T_{reg} fragility and without impacting their maintenance of peripheral tolerance, suggesting that this was a proximally- and locally-driven event, likely induced by inflammation. While we only observed this in the context of the tumor microenvironment, it is possible that T_{reg} fragility could indeed occur in other inflammatory settings where exposure to IFNγ is increased. We would argue that the mechanism of IFNγ-induced T_{reg} fragility is mediated directly between *Nrp1*$^{-/-}$ and WT T_{regs} as either loss of IFNγ or IFNγR expression, respectively, impacts fragility. While it is possible that IFNγ derived from other cell populations, such as $CD8^+$ T cells or NK cells, or the ensuing anti-tumor response and altered tumor microenvironment contributed to T_{reg} fragility, it is noteworthy that the dominant IFNγ-producing cell type was *Nrp1*$^{-/-}$ T_{regs} and $CD8^+$ T cell depletion did not impact the enhanced IFNγ production and loss of suppressive activity observed. [vii] IFNγR expression on intratumoral T_{regs} was required for an effective response to PD1 blockade. Strikingly, *Ifngr1*$^{L/L}$*Foxp3*$^{Cre\text{-}YFP}$ mice were completely resistant to anti-PD1 immunotherapy. Whereas WT T_{regs} showed a significant increase in IFNγ expression after PD1 blockade, *Ifngr1*$^{-/-}$ T_{regs} showed no increase in IFNγ, suggesting that IFNγ-driven T_{reg} fragility may need to be induced for an effective immunotherapeutic response.

A previous study had suggested that the absence of Nrp1 leads to reduced influx of T_{regs} into certain tumor types (*Vegfa*$^{+/+}$ or *Vegfa*$^{-/-}$ fibrosarcomas and *Ret* melanoma models) (Hansen et al., 2012). However, we did not observe any defect in the migration of Nrp1-deficient T_{regs} even in the competitive environment of B16 tumors in heterozygous *Nrp1*$^{L/L}$*Foxp3*$^{Cre\text{-}YFP/DTR\text{-}GFP}$ female mice. These discrepancies could be due to the different tumor models analyzed. Alternatively, their study primarily utilized *Nrp1*$^{L/L}$*CD4*^{Cre} mice in which Nrp1 would be removed in all T cells, which could have many direct and indirect effects on intratumoral T_{regs} (Hansen et al., 2012). Indeed, we and others have shown that Nrp1 is expressed on a number of cell types, especially in the tumor (Jackson et al., 2014) (data not shown).

Whether T_{reg} fragility is a feature of certain diseases and the extent to which this can be prevented or utilized therapeutically remains largely unknown and highly controversial (Rubtsov et al., 2010; Sakaguchi et al., 2013; Zhou et al., 2009a; Zhou et al., 2009b). We speculate that the IFNγ pathway may drive T_{reg} fragility in certain inflammatory environments. The loss of Nrp1 not only results in T_{reg} fragility but also results in substantial IFNγ expression, which in turn induces fragility in other T_{regs} regardless of their Nrp1 expression in a feed-forward manner; a process we refer to as “infectious fragility”. As IFNγ production is a hallmark of a productive T cell-mediated immune response, our observations also raise the possibility that IFNγ-induced T_{reg} fragility may be a physiologically important regulatory mechanism to locally limit T_{reg} function and promote a productive immune response. Given the profound consequences of T_{reg}-derived IFNγ production, our data emphasize the importance of the Nrp1 pathway in limiting T_{reg} fragility in the tumor microenvironment but also highlights that this pathway can be overcome when sufficient IFNγ is induced. Indeed, our data show that the IFNγ response induced by PD1 blockade appears to be sufficient to drive intratumoral T_{reg} fragility despite expression of

Nrp1. However, loss of IFNγR expression on T_{regs}, renders mice completely resistant to anti-PD1 immunotherapy. This raises the provocative possibility that an essential component of effective immunotherapy is to induce sufficient IFNγ in the tumor microenvironment to drive T_{reg} fragility. However, the impact of T_{reg} fragility and IFNγ expression by intratumoral T_{regs} on tumor growth and responsiveness to immunotherapy in murine and human tumors needs to be investigated further.

As a high frequency of intratumoral T_{regs} in cancer patients is largely considered a negative prognostic factor (Facciabene et al., 2012; Ichihara et al., 2003; Knol et al., 2011), identifying approaches to selectively target intratumoral T_{regs} while maintaining peripheral tolerance is critical. Although expression of NRP1 in peripheral, tissue-resident T_{regs} remains unclear, our findings highlight the surprisingly extensive and variable expression of NRP1 on human intratumoral T_{regs} (Battaglia et al., 2009; Battaglia et al., 2008; Chaudhary et al., 2014; Milpied et al., 2009). Importantly, given that our mouse model experiments suggest that NRP1 may not need to be targeted in all human intratumoral T_{regs} to derive a therapeutic effect, it is possible that targeting $NRP1^{+}$ intratumoral T_{regs} with an NRP1 mAb may be therapeutic. As we show that the impact of the IFNγ pathway on human T_{regs} is conserved, it is possible that by blocking NRP1 on T_{regs}, one could induce functional fragility in surrounding T_{regs} to further enhance the therapeutic effect and overall outcome. Our identification of IFNγ as the critical mediator of T_{reg} fragility, whether driven by manipulation of the Nrp1 pathway in T_{regs} or PD1 blockade highlights the potential importance of this mechanism in promoting anti-tumor immunity and provides a pathway to develop immunotherapeutic approaches that could lead to tumor reduction while maintaining peripheral tolerance.

Star Methods

Contact for Reagent and Resource Sharing

Further information and requests for reagents should be directed to and will be fulfilled by the Lead Contact, Dario A.A. Vignali (dvignali@pitt.edu).

Experimental Model and Subject Details

Mice—*Nrp1*$^{L/L}$ mice were obtained from D. Cheresh (UC San Diego). *Foxp3*$^{Cre\text{-}YFP/Cre\text{-}YFP}$, *Foxp3*$^{DTR\text{-}GFP/DTR\text{-}GFP}$, *Foxp3*$^{-/-}$ mice were obtained from A.Y. Rudensky (Memorial Sloan Kettering). (Fontenot et al., 2003; Kim et al., 2007; Rubtsov et al., 2008). *Ifngr1*$^{-/-}$, *Ifng*$^{-/-}$, *Ifngr1*$^{L/L}$ and *Rosa*$^{L\text{-}Tomato\text{-}L\text{-}GFP}$ mice were obtained from Jackson Laboratories (Dalton et al., 1993; Huang et al., 1993; Lee et al., 2013). All animal experiments were performed in the American Association for the Accreditation of Laboratory Animal Care-accredited, specific-pathogen-free facilities in Animal Resource Center, St. Jude Children's Research Hospital (SJCRH), and Division of Laboratory Animal Resources, University of Pittsburgh School of Medicine (UPSOM). Female and male mice were used. Animal protocols were approved by the Institutional Animal Care and Use Committees of SJCRH and UP.

Human T-cell populations—All HNSCC and melanoma tissues were acquired under a University of Pittsburgh Cancer Institute Institutional Review Board (IRB)-approved protocol with written informed consent obtained from each patient in conjunction with the University of Pittsburgh Cancer Institute HNSCC and Melanoma SPOREs. There were no restrictions on cancer subtype, smoking status, age, race, or prior adjuvant therapy. Control donor peripheral blood (PBL) was collected through an approved MTA protocol with the Western Pennsylvania Bloodbank. Human HNSCC PBL and TIL samples (unmatched) as well as healthy donor PBL samples were provided by R. Ferris from patients with high-risk, advanced (stage III or IV) resectable HNSCC treated with surgery. Most tumors were from oral cavity or laryngeal sites, and all were HPV-negative. Tumor specimens were obtained at the time of surgical resection, prior to adjuvant therapy. TIL were isolated, frozen, and thawed prior to staining for NRP1. Freshly processed samples were used in functional assays. Human melanoma TIL and PBL samples were provided by J. Kirkwood from an accrual trail (96-099) of patients with metastatic melanoma.

Method Details

Antibodies and flow cytometry—Single cell suspensions were stained with antibodies against CD4 (clone# GK1.5, Biolegend), CD8a (clone# YTS156.7.7, Biolegend; clone# H35-17.2, eBioscience), TCRβ (clone# H57-597, Biolegend), Thy1.1 (clone# OX-7, Biolegend), Thy1.2 (clone# 30-H12, Biolegend), Foxp3 (clone# FJK-16s, eBioscience; clone# 150D, Biolegend), IFNγ (clone# XMG1.2, Biolegend), ICOS (clone# C398.4A, Biolegend), phosphor-Stat1 (Clone# 4a, BD Biosciences) and phosphor-Stat4 (Clone# 38, BD Biosciences). Surface staining was performed on ice for 15min. For cytokine expression analysis, cells were activated with 0.1ng/ml PMA (Sigma) and 0.5ng/ml Ionomycin (Sigma) in RPMI containing 10% FBS and Monensin (eBioscience) for 8hr. For intracellular staining of cytokines and transcription factors, cells were stained with surface markers, fixed in Fix/Perm buffer (eBioscience) for 15 minutes, washed in permeabilization buffer (eBioscience) twice and stained intracellular factors in permeabilization buffer for 30min on ice. For phosphoprotein staining, cells were fixed with 1.5% PFA (Alfa Aesar) at 37°C for 15min, permeabilized with ice cold Methanol for 1hr, and stained on ice for 1hr. Cells were sorted on Aria II (BD Biosciences) or analyzed on Fortessa (BD Biosciences), and data analysis was performed on FlowJo (Tree Star).

Tumor models—*Foxp3*$^{Cre\text{-}YFP/Cre\text{-}YFP}$, *Nrp1*$^{L/L}$ *Foxp3*$^{Cre\text{-}YFP/Cre\text{-}YFP}$, or *Foxp3*$^{DTR\text{-}GFP/DTR\text{-}GFP}$ mice were injected with B16.F10 melanoma (1.25×10^5 cells intradermally). Tumors were measured every 3 days with digital calipers and tumor size was calculated; this was performed in blinded manner but not randomized. 100ug Diptheria Toxin was injected every 3 days starting on day 7 in *Foxp3*$^{DTR\text{-}GFP/DTR\text{-}GFP}$ and *Foxp3*$^{DTR\text{-}GFP/+}$ mice. Sema4aIg was injected every 3 days starting on day 5 (400ug, 200ug, 200ug), and anti-CD8 (YTS) was injected every 3 days starting on day 5 (200ug). *Foxp3*$^{Cre\text{-}YFP}$ and *Ifngr1*$^{L/L}$ *Foxp3*$^{Cre\text{-}YFP}$ mice were injected with MC38 (5×10^5 cells subcutaneously). Tumors were measured as above and mice were treated with either anti-PD1 (clone G4) or isotype (Armenian Hamster IgG). Tumors and non-tumor draining lymph nodes were collected for analysis on day 12. TILs were prepared with enzymatic (collagenase IV and dispase, 1mg/mL) and mechanical disruption. To achieve reasonable

power, at least 5 mice were used in each group, at least 3 mice per group per experiment. Group means were compared with Student's t tests. Tumor growth over time was analyzed using two-way ANOVA with multiple comparisons. Event-free survival (moribund) estimates were calculated with the Kaplan-Meier method. Groups of mice were compared by log-rank test. All p values are two-sided, and statistical significance was assessed at the 0.05 level. Analyses were conducted using GraphPad Prism software.

Foxp3$^{-/-}$ model—*CD45.1*$^{+}$ *Foxp3*$^{+/-}$ female mice were bred with *CD45.1*$^{+}$*Foxp3*$^{+/+}$ male mice in timed matings. Male progeny were genotyped at birth for *Foxp3*$^{-/-}$ status. T_{regs} from *Thy1.1*$^{+}$ *Foxp3*$^{Cre\text{-}YFP/Cre\text{-}YFP}$, *Thy1.2*$^{+}$ *Nrp1*$^{L/L}$*Foxp3*$^{Cre\text{-}YFP/Cre\text{-}YFP}$, *Thy1.2*$^{+}$ *Ifng*$^{-/-}$*Nrp1*$^{L/L}$*Foxp3*$^{Cre\text{-}YFP/Cre\text{-}YFP}$, *Thy1.1*$^{+}$ *Ifngr1*$^{-/-}$ *Foxp3*$^{Cre\text{-}YFP/Cre\text{-}YFP}$ mice were purified by FACS and 10^6 cells injected intraperitoneally into *Foxp3*$^{-/-}$ male pups within 2 days of birth (Workman et al., 2011). When a 50:50 mixture of T_{regs} was injected the total was maintained at 10^6 cells. Mice were monitored for the autoimmune phenotype ‘scurfy’ (scaly skin, eye inflammation, runted phenotype, and lack of mobility) (Workman et al., 2011). Any mice exhibiting any autoimmune or inflammatory symptoms prior to B16 injection, even if mild, were removed from further study. Mice were injected with 1.25×10^5 B16.F10 cells at 4 weeks of age and tumor growth was monitored every 3 days.

Gene expression profiling by RNAseq and bioinformatics analyses—Tregs (5×10^3) were either single (n=3) or double sorted (n=2) and cDNAs were prepared using the SMARTer® Ultra™ Low Input RNA Kit for Sequencing - v3 user manual (Clontech Laboratories). We reasoned that double sorting results in higher purity but has lower yield and may alter the expression profile. Though melanoma genes were found at lower levels in double sorted samples no other substantial differences, such as activation of stress response genes, were observed. T_{regs} were sorted on the following markers: Foxp3$^{Cre\text{-}YFP/Cre\text{-}YFP}$ (Nrp1$^{+/+}$) on YFP, Nrp1$^{L/L}$Foxp3$^{Cre\text{-}YFP/Cre\text{-}YFP}$ (Nrp1$^{-/-}$) on YFP, Nrp1$^{L/L}$Foxp3$^{Cre\text{-}YFP/DTR\text{-}GFP}$ (Nrp1$^{-/-}$) on YFP, and Nrp1$^{L/L}$Foxp3$^{Cre\text{-}YFP/DTR\text{-}GFP}$ (Nrp1$^{+/+}$) on GFP. Sequencing libraries were prepared using Nextera XT DNA Library Preparation kit (Illumina), normalized at 2nM using Tris-HCl (10mM, pH 8.5) with 0.1% Tween20, diluted and denatured to a final concentration of 1.8nM using the Illumina Denaturing and Diluting libraries for the NextSeq 500 protocol Revision D (Illumina). Cluster generation and 75bp paired-end dual-indexed sequencing was performed on Illumina NextSeq 500 system.

RNAseq data was aligned to the mm10 genome using the STAR aligner (Dobin et al., 2013) and quantified using featureCounts (Liao et al., 2014). The raw counts data were processed using the “voom” function (Law et al., 2014) in the limma R package (Ritchie et al., 2015; Wu and Smyth, 2012), which normalizes the data and assigns a weight for each measurement for subsequent linear model fitting. Unsupervised analysis of the date revealed a small cluster of melanoma specific genes that reasoned were caused by contaminations. Following a previous approach (Battle et al., 2014), we removed five melanoma specific genes from all downstream analysis (Mlana, Syt4, Tyr, Tyrp1, Dct). To filter for low expression genes we defined a cutoff of 90 reads per gene based on visual inspection of the bimodal count distribution. Only genes that meat this threshold in at least 5 samples

(~11,000 out of ~23,000) were kept for further analysis. Differential expression was assessed using the limma moderated T statistic. The differences between the intratumoral Treg populations were subtle and in order to increase the power of our study we included technical factors as covariates in our differential expression analysis. Following the approach outlined in a recent human RNAseq study (Battle et al., 2014) we included three Picard RNAseq metrics ("PCT_INTERGENIC_BASES" "MEDIAN_3PRIME_BIAS", "MEDIAN_CV_COVERAGE") (Picard) as well GC correlation (computed as the sample specific Pearson correlation between each gene's GC content and its expression value). Normalization for replicate number and technical parameters was also applied directly to the voom result to obtain "normalized counts", which were used for data visualization. Geneset enrichment was performed using the "RankSumWithCorrelation" function in the limma R package, which automatically corrects enrichment statistic inflation due to correlation among genes (with the immune genesets restricted to those relevant to T cells). p-values were combined from the "*Nrp1*$^{L/L}$*Foxp3*$^{Cre\text{-}YFP/Cre\text{-}YFP}$ (Nrp1$^{-/-}$) vs *Foxp3*$^{Cre\text{-}YFP/Cre\text{-}YFP}$ (Nrp1$^{+/+}$)" and "*Nrp1*$^{L/L}$*Foxp3*$^{Cre\text{-}YFP/DTR\text{-}GFP}$ (Nrp1$^{+/+}$) vs *Nrp1*$^{L/L}$*Foxp3*$^{Cre\text{-}YFP/DTR\text{-}GFP}$ (Nrp1$^{-/-}$) using the Fisher's "log sum" method [Fisher] to define significant genes. Genesets with a q-value FDR of <0.2 were considered significant. In order to assess the alterations in Treg specific expression profile we relied on the Treg signature genes defined in a previous study (Hill et al., 2007). For pathway analysis bar charts, results of geneset enrichment analysis were depicted with colors representing the effect size and height representing the corresponding p-values. The effect size is defined as AUC (area under receiver operating curve) – 0.5 which provides a normalized ranksum statistic that is comparable across genesets of different sizes. The plot is restricted to the top 10 pathways (based on their Nrp1$^{+/+}$ vs Nrp1$^{-/-}$ significance) from the "canonical" mSigDB geneset. We additionally restricted this analysis to genesets and pathways that were deemed relevant to intercellular signaling (defined at least half of the genes in the geneset having an extracellular or membrane annotation).

***In vitro* assays—**Splenic CD4^{+}YFP^{-} (CD4^{+}Foxp3^{-} T cells) cells from *Foxp3*$^{Cre\text{-}YFP}$ mice were sorted as responder cells and labeled with 5μM CellTrace Violet (Life Technology). CD4^{-}CD8^{-} splenocytes from *Foxp3*$^{Cre\text{-}FP}$ mice were treated with 20μg/mL mytomycin C (Sigma) at 37°C for 30min, washed five times with PBS, and then used as antigen presenting cells (APCs). Responder cells (4×10^3), APCs (8×10^3), and different concentrations of T_{regs} (1:2-1:16 T_{reg}:$T_e$ff ratio, 500-2000 T_{regs}) were activated with 2μg/ml anti-CD3 (Biolegend) in a 96-well round bottom plate with 100ul RPMI for 3 days (Turnis et al., 2016). Suppression was calculated as previously described (McMurchy and Levings, 2012). Briefly, cells were acquired by BD Fortessa, and the division index of responder cells was analyzed using FlowJo based on the division of CellTrace Violet. Suppression was then calculated with the formula % Suppression = (1-DIT_{reg}/DICtrl) × 100% (DIT_{reg} stands for the division index of responder cells with Tregs, and DICtrl stands for the division index of responder cells activated without T_{regs}). Human microsuppression assays were performed similarly to mouse assays with the following changes: 0.5μg/ml anti-CD3 is used for activation, and cells are cultured in assay conditions (200uL) for 4 days.

For co-culture assays, sorted T_{reg} populations were cultured together in a 96 well round-bottom plate or in a 96 well transwell plate (Millipore) for 72 hours prior to being resorted and used in a suppression assay. Cells were treated with 100ng/mL PMA (Sigma), 500ng/mL Ionomycin (Sigma) and 10001U hIL-2 (Prometheus) for co-culture. For some experiments, sorted T_{regs} were cultured in the presence of 0.3-20ng/mL anti-IFNγ (BioXcell) or 0-200ng/mL IFNγ (Biolegend) to the microsuppression assay.

For the hypoxia assays, T_{regs} were stimulated with PMA/Ionomycin and IL-2 for 3 days in normoxic (5% CO_2 and 20% O_2) or hypoxic (5.5% CO_2 and 1.5% O_2) conditions at 37°C. Cells were then stained in the same condition in the absence of cytokine.

Quantification and Statistical Analysis

Statistics were performed using Prism v6.07. Student t tests were used in Figures 1B,H; 3B-E; 4B-D, F-G; 5B,D; 7B-C and supplemental figures 1A-B; 2E-F, 5, 6B-D, 7C. ANOVA was used in Figures 1C, E, G; 5E-G; 6; 7A. Kaplan Meier was used in Figures 1C, E, F; 7A. “n” represents the number of mice used in the experiment, with the number of individual experiments listed in the legend. Graphs show individual samples. Samples are shown with the mean with or without error bars showing the SEM. Significance was defined as p=0.05.

Data and Software Availability

The RNASeq datasets have been deposited in the Gene Expression Omnibus (GEO) under code GSE97939.

Supplementary Material

Refer to Web version on PubMed Central for supplementary material.

Acknowledgments

The authors would like to thank A. Rudensky and D. Cheresh for mice, A. Yates, D. Falkner, H. Shen from the Immunology Flow Core for cell sorting, the staff of the Division of Laboratory Animal Services for the animal husbandry, and the Immunology Department at the University of Pittsburgh for helpful discussions. This work was supported by the National Institutes of Health (R01 AI091977 to D.A.A.V.; F31 CA189441 to A.E.O.), NCI Comprehensive Cancer Center Support CORE grant (CA047904 and CA21765, to D.A.A.V.), and the American Lebanese Syrian Associated Charities (ALSAC, to D.A.A.V.). Part of this project used the UPCI Flow Core that is supported in part by P30 CA047904.

References

Battaglia A, Buzzonetti A, Baranello C, Ferrandina G, Martinelli E, Fanfani F, Scambia G, Fattorossi A. Metastatic tumour cells favour the generation of a tolerogenic milieu in tumour draining lymph node in patients with early cervical cancer. Cancer immunology, immunotherapy : CII. 2009; 58:1363–1373. [PubMed: 19172271]

Battaglia A, Buzzonetti A, Monego G, Peri L, Ferrandina G, Fanfani F, Scambia G, Fattorossi A. Neuropilin-1 expression identifies a subset of regulatory T cells in human lymph nodes that is modulated by preoperative chemoradiation therapy in cervical cancer. Immunology. 2008; 123:129–138. [PubMed: 18028372]

Battle A, Mostafavi S, Zhu X, Potash JB, Weissman MM, McCormick C, Haudenschild CD, Beckman KB, Shi J, Mei R, et al. Characterizing the genetic basis of transcriptome diversity through RNA-sequencing of 922 individuals. Genome research. 2014; 24:14–24. [PubMed: 24092820]

Briggs SF, Reijo Pera RA. X chromosome inactivation: recent advances and a look forward. Current opinion in genetics & development. 2014; 28:78–82. [PubMed: 25461454]

Chaudhary B, Elkord E. Novel expression of Neuropilin 1 on human tumor-infiltrating lymphocytes in colorectal cancer liver metastases. Expert opinion on therapeutic targets. 2015; 19:147–161. [PubMed: 25351619]

Chaudhary B, Khaled YS, Ammori BJ, Elkord E. Neuropilin 1: function and therapeutic potential in cancer. Cancer immunology, immunotherapy : CII. 2014; 63:81–99. [PubMed: 24263240]

Chaudhry A, Rudensky AY. Control of inflammation by integration of environmental cues by regulatory T cells. J Clin Invest. 2013; 123:939–944. [PubMed: 23454755]

Curiel TJ, Coukos G, Zou L, Alvarez X, Cheng P, Mottram P, Evdemon-Hogan M, Conejo-Garcia JR, Zhang L, Burow M, et al. Specific recruitment of regulatory T cells in ovarian carcinoma fosters immune privilege and predicts reduced survival. Nat Med. 2004; 10:942–949. [PubMed: 15322536]

Dalton DK, Pitts-Meek S, Keshav S, Figari IS, Bradley A, Stewart TA. Multiple defects of immune cell function in mice with disrupted interferon-gamma genes. Science. 1993; 259:1739–1742. [PubMed: 8456300]

Dang EV, Barbi J, Yang HY, Jinasena D, Yu H, Zheng Y, Bordman Z, Fu J, Kim Y, Yen HR, et al. Control of T(H)17/T(reg) balance by hypoxia-inducible factor 1. Cell. 2011; 146:772–784. [PubMed: 21871655]

Delgoffe GM, Woo SR, Turnis ME, Gravano DM, Guy C, Overacre AE, Bettini ML, Vogel P, Finkelstein D, Bonnevier J, et al. Stability and function of regulatory T cells is maintained by a neuropilin-1-semaphorin-4a axis. Nature. 2013

Deligne C, Metidji A, Fridman WH, Teillaud JL. Anti-CD20 therapy induces a memory Th1 response through the IFN-gamma/IL-12 axis and prevents protumor regulatory T-cell expansion in mice. Leukemia. 2015; 29:947–957. [PubMed: 25231744]

Dobin A, Davis CA, Schlesinger F, Drenkow J, Zaleski C, Jha S, Batut P, Chaisson M, Gingeras TR. STAR: ultrafast universal RNA-seq aligner. Bioinformatics (Oxford, England). 2013; 29:15–21.

Dominguez-Villar M, Baecher-Allan CM, Hafler DA. Identification of T helper type 1-like, Foxp3+ regulatory T cells in human autoimmune disease. Nat Med. 2011; 17:673–675. [PubMed: 21540856]

Drennan S, Stafford ND, Greenman J, Green VL. Increased frequency and suppressive activity of CD127(low/-) regulatory T cells in the peripheral circulation of patients with head and neck squamous cell carcinoma are associated with advanced stage and nodal involvement. Immunology. 2013; 140:335–343. [PubMed: 23826668]

Duhen T, Duhen R, Lanzavecchia A, Sallusto F, Campbell DJ. Functionally distinct subsets of human FOXP3+ Treg cells that phenotypically mirror effector Th cells. Blood. 2012; 119:4430–4440. [PubMed: 22438251]

Facciabene A, Motz GT, Coukos G. T-regulatory cells: key players in tumor immune escape and angiogenesis. Cancer Res. 2012; 72:2162–2171. [PubMed: 22549946]

Fontenot JD, Gavin MA, Rudensky AY. Foxp3 programs the development and function of CD4+CD25+ regulatory T cells. Nat Immunol. 2003; 4:330–336. [PubMed: 12612578]

Fontenot JD, Rasmussen JP, Williams LM, Dooley JL, Farr AG, Rudensky AY. Regulatory T cell lineage specification by the forkhead transcription factor foxp3. Immunity. 2005; 22:329–341. [PubMed: 15780990]

Galupa R, Heard E. X-chromosome inactivation: new insights into cis and trans regulation. Current opinion in genetics & development. 2015; 31:57–66. [PubMed: 26004255]

Gao YL, Chai YF, Qi AL, Yao Y, Liu YC, Dong N, Wang LJ, Yao YM. Neuropilin-1highCD4(+)CD25(+) Regulatory T Cells Exhibit Primary Negative Immunoregulation in Sepsis. Mediators of inflammation. 2016; 2016:7132158. [PubMed: 27239104]

Hansen W, Hutzler M, Abel S, Alter C, Stockmann C, Kliche S, Albert J, Sparwasser T, Sakaguchi S, Westendorf AM, et al. Neuropilin 1 deficiency on CD4+Foxp3+ regulatory T cells impairs mouse melanoma growth. The Journal of experimental medicine. 2012; 209:2001–2016. [PubMed: 23045606]

Hill JA, Feuerer M, Tash K, Haxhinasto S, Perez J, Melamed R, Mathis D, Benoist C. Foxp3 transcription-factor-dependent and -independent regulation of the regulatory T cell transcriptional signature. Immunity. 2007; 27:786–800. [PubMed: 18024188]

Hori S. Lineage stability and phenotypic plasticity of Foxp3(+) regulatory T cells. Immunol Rev. 2014; 259:159–172. [PubMed: 24712465]

Huang S, Hendriks W, Althage A, Hemmi S, Bluethmann H, Kamijo R, Vilcek J, Zinkernagel RM, Aguet M. Immune response in mice that lack the interferon-gamma receptor. Science. 1993; 259:1742–1745. [PubMed: 8456301]

Ichihara F, Kono K, Takahashi A, Kawaida H, Sugai H, Fujii H. Increased populations of regulatory T cells in peripheral blood and tumor-infiltrating lymphocytes in patients with gastric and esophageal cancers. Clin Cancer Res. 2003; 9:4404–4408. [PubMed: 14555512]

Jackson SR, Berrien-Elliott M, Yuan J, Hsueh EC, Teague RM. Neuropilin-1 expression is induced on tolerant self-reactive CD8+ T cells but is dispensable for the tolerant phenotype. PLoS One. 2014; 9:e110707. [PubMed: 25343644]

Jacobs JF, Nierkens S, Figdor CG, de Vries IJ, Adema GJ. Regulatory T cells in melanoma: the final hurdle towards effective immunotherapy? The Lancet Oncology. 2012; 13:e32–42. [PubMed: 22225723]

Kim JM, Rasmussen JP, Rudensky AY. Regulatory T cells prevent catastrophic autoimmunity throughout the lifespan of mice. Nat Immunol. 2007; 8:191–197. [PubMed: 17136045]

Knol AC, Nguyen JM, Quereux G, Brocard A, Khammari A, Dreno B. Prognostic value of tumor-infiltrating Foxp3+ T-cell subpopulations in metastatic melanoma. Experimental dermatology. 2011; 20:430–434. [PubMed: 21410773]

Koch MA, Thomas KR, Perdue NR, Smigiel KS, Srivastava S, Campbell DJ. T-bet(+) Treg cells undergo abortive Th1 cell differentiation due to impaired expression of IL-12 receptor beta2. Immunity. 2012; 37:501–510. [PubMed: 22960221]

Koenecke C, Lee CW, Thamm K, Fohse L, Schafferus M, Mittrucker HW, Floess S, Huehn J, Ganser A, Forster R, et al. IFN-gamma production by allogeneic Foxp3+ regulatory T cells is essential for preventing experimental graft-versus-host disease. J Immunol. 2012; 189:2890–2896. [PubMed: 22869903]

Law CW, Chen Y, Shi W, Smyth GK. voom: Precision weights unlock linear model analysis tools for RNA-seq read counts. Genome biology. 2014; 15:R29. [PubMed: 24485249]

Lee JH, Elly C, Park Y, Liu YC. E3 Ubiquitin Ligase VHL Regulates Hypoxia-Inducible Factor-1alpha to Maintain Regulatory T Cell Stability and Suppressive Capacity. Immunity. 2015; 42:1062–1074. [PubMed: 26084024]

Lee JT, Bartolomei MS. X-inactivation, imprinting, and long noncoding RNAs in health and disease. Cell. 2013; 152:1308–1323. [PubMed: 23498939]

Lee SH, Carrero JA, Uppaluri R, White JM, Archambault JM, Lai KS, Chan SR, Sheehan KC, Unanue ER, Schreiber RD. Identifying the initiating events of anti-Listeria responses using mice with conditional loss of IFN-gamma receptor subunit 1 (IFNGR1). J Immunol. 2013; 191:4223–4234. [PubMed: 24048899]

Liao Y, Smyth GK, Shi W. featureCounts: an efficient general purpose program for assigning sequence reads to genomic features. Bioinformatics (Oxford, England). 2014; 30:923–930.

Liu C, Workman CJ, Vignali DA. Targeting regulatory T cells in tumors. The FEBS journal. 2016; 283:2731–2748. [PubMed: 26787424]

McMurchy AN, Levings MK. Suppression assays with human T regulatory cells: a technical guide. Eur J Immunol. 2012; 42:27–34. [PubMed: 22161814]

Milpied P, Renand A, Bruneau J, Mendes-da-Cruz DA, Jacquelin S, Asnafi V, Rubio MT, MacIntyre E, Lepelletier Y, Hermine O. Neuropilin-1 is not a marker of human Foxp3+ Treg. Eur J Immunol. 2009; 39:1466–1471. [PubMed: 19499532]

Miyara M, Sakaguchi S. Natural regulatory T cells: mechanisms of suppression. Trends in molecular medicine. 2007; 13:108–116. [PubMed: 17257897]

Nishikawa H, Sakaguchi S. Regulatory T cells in tumor immunity. International journal of cancer Journal international du cancer. 2010; 127:759–767. [PubMed: 20518016]

Olalekan SA, Cao Y, Hamel KM, Finnegan A. B cells expressing IFN-gamma suppress Treg-cell differentiation and promote autoimmune experimental arthritis. Eur J Immunol. 2015; 45:988–998. [PubMed: 25645456]

Oldenhove G, Bouladoux N, Wohlfert EA, Hall JA, Chou D, Dos Santos L, O'Brien S, Blank R, Lamb E, Natarajan S, et al. Decrease of Foxp3+ Treg cell number and acquisition of effector cell phenotype during lethal infection. Immunity. 2009; 31:772–786. [PubMed: 19896394]

Overacre AE, Vignali DA. Treg stability: to be or not to be. Curr Opin Immunol. 2016; 39:39–43. [PubMed: 26774863]

Pandiyan P, Zhu J. Origin and functions of pro-inflammatory cytokine producing Foxp3+ regulatory T cells. Cytokine. 2015; 76:13–24. [PubMed: 26165923]

Picard. picard. In Picard (Broad Institute).

Piechnik A, Dmoszynska A, Omiotek M, Mlak R, Kowal M, Stilgenbauer S, Bullinger L, Giannopoulos K. The VEGF receptor, neuropilin-1, represents a promising novel target for chronic lymphocytic leukemia patients. International journal of cancer Journal international du cancer. 2013; 133:1489–1496. [PubMed: 23447383]

Ritchie ME, Phipson B, Wu D, Hu Y, Law CW, Shi W, Smyth GK. limma powers differential expression analyses for RNA-sequencing and microarray studies. Nucleic acids research. 2015; 43:e47. [PubMed: 25605792]

Rubtsov YP, Niec RE, Josefowicz S, Li L, Darce J, Mathis D, Benoist C, Rudensky AY. Stability of the regulatory T cell lineage in vivo. Science. 2010; 329:1667–1671. [PubMed: 20929851]

Rubtsov YP, Rasmussen JP, Chi EY, Fontenot J, Castelli L, Ye X, Treuting P, Siewe L, Roers A, Henderson WR Jr, et al. Regulatory T cell-derived interleukin-10 limits inflammation at environmental interfaces. Immunity. 2008; 28:546–558. [PubMed: 18387831]

Saito T, Nishikawa H, Wada H, Nagano Y, Sugiyama D, Atarashi K, Maeda Y, Hamaguchi M, Ohkura N, Sato E, et al. Two FOXP3(+)CD4(+) T cell subpopulations distinctly control the prognosis of colorectal cancers. Nat Med. 2016; 22:679–684. [PubMed: 27111280]

Sakaguchi S, Vignali DA, Rudensky AY, Niec RE, Waldmann H. The plasticity and stability of regulatory T cells. Nat Rev Immunol. 2013; 13:461–467. [PubMed: 23681097]

Sharma MD, Huang L, Choi JH, Lee EJ, Wilson JM, Lemos H, Pan F, Blazar BR, Pardoll DM, Mellor AL, et al. An inherently bifunctional subset of Foxp3+ T helper cells is controlled by the transcription factor eos. Immunity. 2013; 38:998–1012. [PubMed: 23684987]

St Rose MC, Taylor RA, Bandyopadhyay S, Qui HZ, Hagymasi AT, Vella AT, Adler AJ. CD134/CD137 dual costimulation-elicited IFN-gamma maximizes effector T-cell function but limits Treg expansion. Immunology and cell biology. 2013; 91:173–183. [PubMed: 23295363]

Tatura R, Zeschnigk M, Hansen W, Steinmann J, Vidigal PG, Hutzler M, Pastille E, Westendorf AM, Buer J, Kehrmann J. Relevance of Foxp3(+) regulatory T cells for early and late phases of murine sepsis. Immunology. 2015; 146:144–156. [PubMed: 26059660]

Turnis ME, Sawant DV, Szymczak-Workman AL, Andrews LP, Delgoffe GM, Yano H, Beres AJ, Vogel P, Workman CJ, Vignali DA. Interleukin-35 Limits Anti-Tumor Immunity. Immunity. 2016; 44:316–329. [PubMed: 26872697]

Vignali DA, Collison LW, Workman CJ. How regulatory T cells work. Nat Rev Immunol. 2008; 8:523–532. [PubMed: 18566595]

Visperas A, Shen B, Min B. gammadelta T cells restrain extrathymic development of Foxp3+-inducible regulatory T cells via IFN-gamma. Eur J Immunol. 2014; 44:2448–2456. [PubMed: 24799116]

Workman CJ, Collison LW, Bettini M, Pillai MR, Rehg JE, Vignali DA. In vivo Treg suppression assays. Methods Mol Biol. 2011; 707:119–156. [PubMed: 21287333]

Wu D, Smyth GK. Camera: a competitive gene set test accounting for inter-gene correlation. Nucleic acids research. 2012; 40:e133. [PubMed: 22638577]

Zhao J, Zhao J, Fett C, Trandem K, Fleming E, Perlman S. IFN-gamma- and IL-10-expressing virus epitope-specific Foxp3(+) T reg cells in the central nervous system during encephalomyelitis. The Journal of experimental medicine. 2011; 208:1571–1577. [PubMed: 21746812]

Zhao J, Zhao J, Perlman S. Differential effects of IL-12 on Tregs and non-Treg T cells: roles of IFN-gamma, IL-2 and IL-2R. PLoS One. 2012; 7:e46241. [PubMed: 23029447]

Zhou X, Bailey-Bucktrout S, Jeker LT, Bluestone JA. Plasticity of CD4(+) FoxP3(+) T cells. Curr Opin Immunol. 2009a; 21:281–285. [PubMed: 19500966]

Zhou X, Bailey-Bucktrout SL, Jeker LT, Penaranda C, Martinez-Llordella M, Ashby M, Nakayama M, Rosenthal W, Bluestone JA. Instability of the transcription factor Foxp3 leads to the generation of pathogenic memory T cells in vivo. Nat Immunol. 2009b; 10:1000–1007. [PubMed: 19633673]

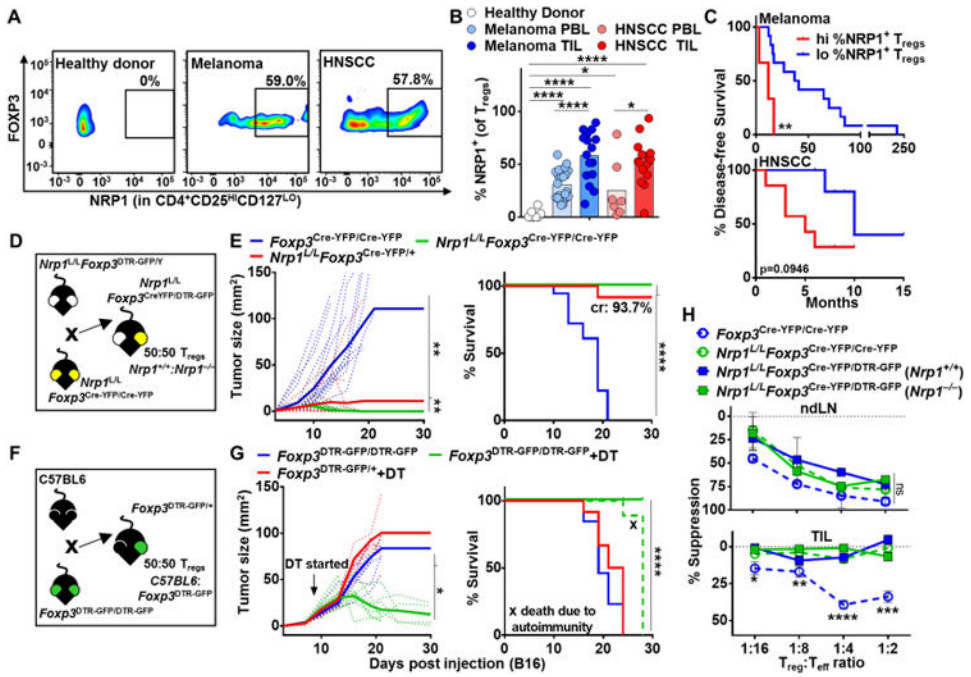

Figure 1. Decreased Nrp1 expression leads to tumor regression and enhanced survival

(**A-C**) Lymphocytes were harvested from PBL of healthy donors (n=8) or from PBL and TIL of Head and Neck Squamous Cell Carcinoma (HNSCC) and metastatic melanoma (3-5 experiments, n=16-23) and frozen or stained fresh. Frozen TIL and PBL were thawed and stained directly without stimulation. (**D-G**) *Foxp3*$^{\text{Cre-YFP/Cre-YFP}}$, *Nrp1*$^{\text{L/L}}$*Foxp3*$^{\text{Cre-YFP/Cre-YFP}}$, *Nrp1*$^{\text{L/L}}$*Foxp3*$^{\text{Cre-YFP/DTR-GFP}}$, *Foxp3*$^{\text{DTR-GFP/DTR-GFP}}$, and *Foxp3*$^{\text{DTR-GFP/+}}$ mice were injected with B16.F10 melanoma tumor cells ID on day 0. Tumor growth was measured with digital calipers every three days. Mice were removed from study when tumor growth reached a diameter of 2cm in any direction or when necrosis was observed, and survival plots were generated (4 experiments, n=9-18). (**F-G**) *Foxp3*$^{\text{DTR-GFP/DTR-GFP}}$, and *Foxp3*$^{\text{DTR-GFP/+}}$ mice were treated with 100μg Diptheria Toxin IP every three days starting on day 7. (**H**) T_{regs} were isolated on day 12 post B16 injection from ndLN and TIL of *Foxp3*$^{\text{Cre-YFP/Cre-YFP}}$, *Nrp1*$^{\text{L/L}}$*Foxp3*$^{\text{Cre-YFP/Cre-YFP}}$, and *Nrp1*$^{\text{L/L}}$*Foxp3*$^{\text{Cre-YFP/DTR-GFP}}$ mice and cultured with effector T cells and APCs for 72 hours in a classical microsuppression assay. T_{regs} were pooled from 3 mice with 5-6 mice per group per experiment. Proliferation was measured and percent suppression was calculated as described in methods. Data represent 3-5 (A-C), 4 (D-G), or 3 (H) independent experiments. Error bars represent the mean ± SEM. Student unpaired t test (Fig. 1B, H), 2 way ANOVA (Fig. 1E, G), and Kaplan-Meier tests (Fig. 1E, G) were used (*$p < 0.05$, **$p < 0.01$, ***$p < 0.001$, ****$p < 0.0001$).

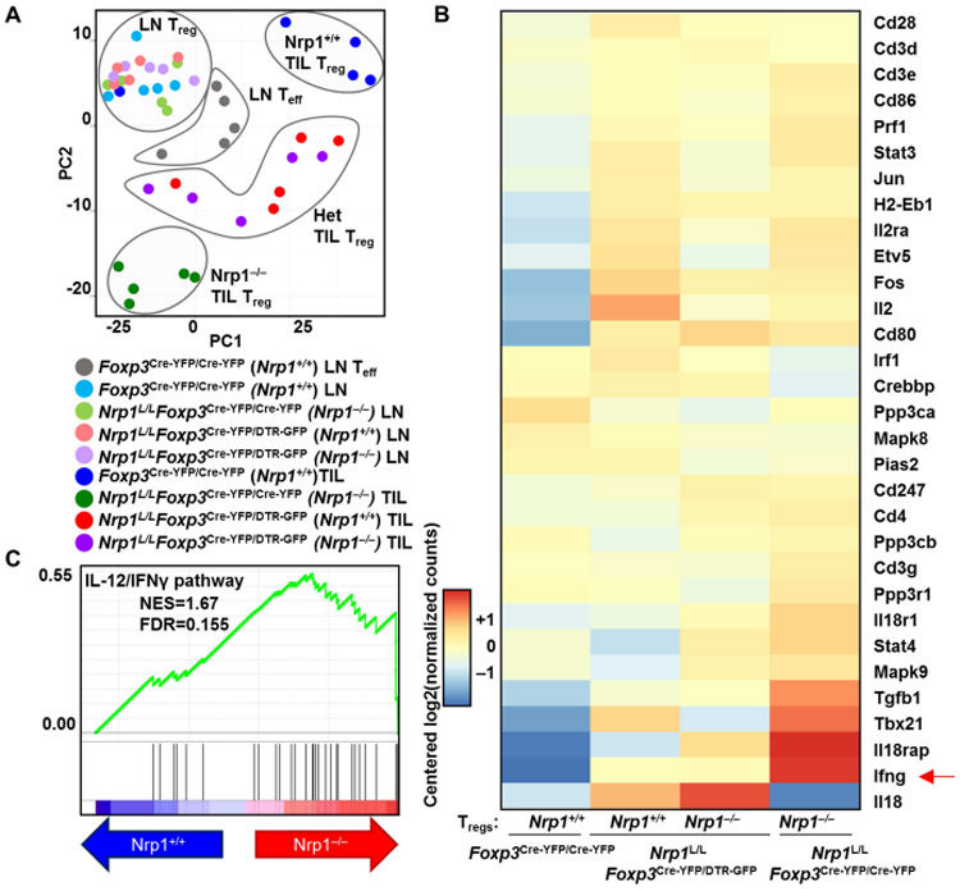

Figure 2. Nrp1 alters the T_{reg} transcriptome

(**A-C**) T_{regs} were purified based on $CD4^+$, and GFP or YFP expression from *Foxp3*$^{Cre\text{-}YFP/Cre\text{-}YFP}$, *Nrp1*$^{L/L}$*Foxp3*$^{Cre\text{-}YFP/Cre\text{-}YFP}$, and *Nrp1*$^{L/L}$*Foxp3*$^{Cre\text{-}YFP/DTR\text{-}GFP}$ mice on D12, cDNA and libraries were generated using the Clontech SmartER Ultra-Low and Illumina Nextera XT Library Prep kits. Samples were normalized to 2nM and sequenced on a NextSeq500. (**A**) Differentially expressed genes are determined by the genes that have q-value of 0.2 between any two of the four T_{reg} groups in the TIL. PCA was computed using the "prcomp()" R functions using the normalized voom data restricted to the same differentially expressed genes as shown in figure. (**B-C**) Significant genes were cross-referenced with those that were annotated to "plasma membrane" or "extracellular part" in the Cellular Component Gene Ontology. The Gene Ontology annotations were obtained from mSigDB. A number of genes associated with the Ifng/Il12/Il18 pathways were upregulated in the *Nrp1*$^{-/-}$ samples. Data represent 5 independent experiments with 3-5 mice pooled per experiment.

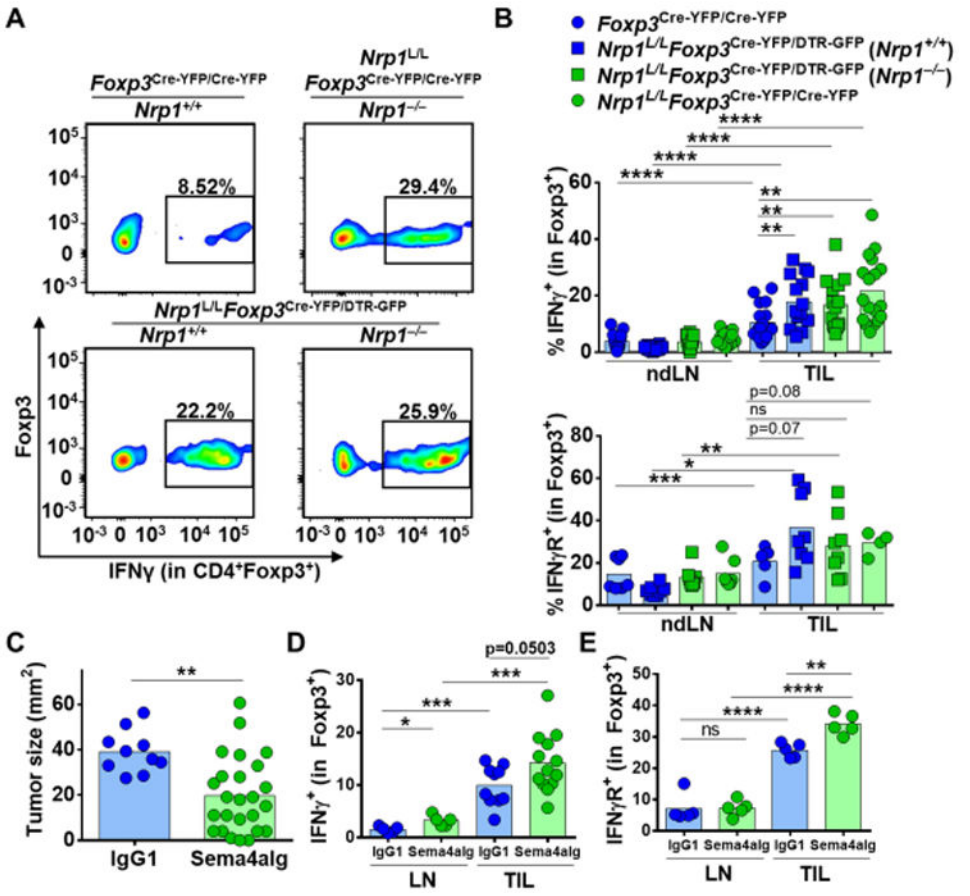

Figure 3. *Nrp1*$^{-/-}$ T_{regs} display increased IFNγ in the tumor microenvironment

(**A-B**) *Foxp3*$^{Cre\text{-}YFP/Cre\text{-}YFP}$, *Nrp1*$^{L/L}$*Foxp3*$^{Cre\text{-}YFP/Cre\text{-}YFP}$, and *Nrp1*$^{L/L}$*Foxp3*$^{Cre\text{-}YFP/DTR\text{-}GFP}$ mice were injected with B16.F10 melanoma tumor cells ID on day 0 and sacrificed on day 12. Lymphocytes were isolated from ndLN and TIL of mice noted, stimulated and stained for IFNγ and IFNγR. (n=8-18). (**C-E**) C57BL/6 mice were injected with B16.F10 melanoma tumor cells ID on day 0. Mice were treated with either Sema4aIg or IgG1 every 3 days until sacrifice starting on day 5 (400ug, 200ug, 200ug, 200ug). (**C**) Tumors were measured on day 12 for prior to sacrifice (n=10-25). (**D**) Lymphocytes were isolated from ndLN and TIL, stimulated and stained for IFNγ (n=5-13). (**E**) Lymphocytes were isolated from ndLN and TIL, and stained for IFNγR (n=5). Data represent 3-4 independent experiments. Student unpaired t test was used. (*p<0.05, **p < 0.01, ***p <0.001, ****p < 0.0001).

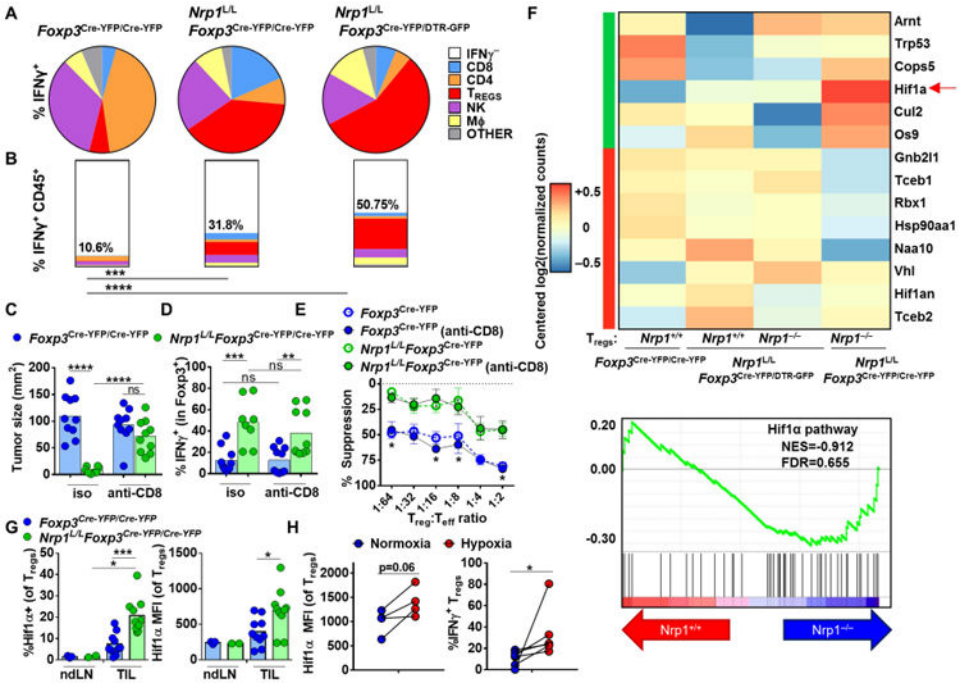

Figure 4. Hypoxia sensitizes intratumoral T_{regs} to IFNγ-mediated fragility

(**A-B**) *Foxp3*$^{Cre\text{-}YFP/Cre\text{-}YFP}$, *Nrp1*$^{L/L}$*Foxp3*$^{Cre\text{-}YFP/Cre\text{-}YFP}$, and *Nrp1*$^{L/L}$*Foxp3*$^{Cre\text{-}YFP/DTR\text{-}GFP}$ mice were injected with B16.F10 melanoma tumor cells ID on day 0 and sacrificed on day 12. Lymphocytes were isolated from TIL of mice noted, stimulated and stained for IFNγ (n=5). (**C-D**) Mice were treated with anti-CD8 or isotype (200ug) every 3 days starting on day 5. Tumor size was measured on day of sacrifice (D12), lymphocytes were isolated from TIL of mice noted, stimulated, and stained for IFNγ (n=7-10). (**E**) Lymphocytes were isolated from mice noted and used in a microsuppression assay. (**F**) T_{regs} were purified, processed, and analyzed as in Fig. 2 (n=5). Heatmap includes genes previously shown to be positive or negative regulators in the Hif1α pathway. Pathway analysis includes all genes in pathway. (**G**) *Foxp3*$^{Cre\text{-}YFP/Cre\text{-}YFP}$ and *Nrp1*$^{L/L}$*Foxp3*$^{Cre\text{-}YFP/Cre\text{-}YFP}$ mice were injected with B16.F10 melanoma tumor cells ID on day 0 and sacrificed on day 12. Lymphocytes were isolated from ndLN and TIL and stained for Hif1α (n=10). (**H**) T_{regs} were isolated from LN of *Foxp3*$^{Cre\text{-}YFP/Cre\text{-}YFP}$ mice, stimulated for 3 days in hypoxia or normoxia, and stained (n=4-6). Data represent 2-5 independent experiments. Student unpaired t test was used. (*p<0.05, **p < 0.01, ***p < 0.001, ****p < 0.0001).

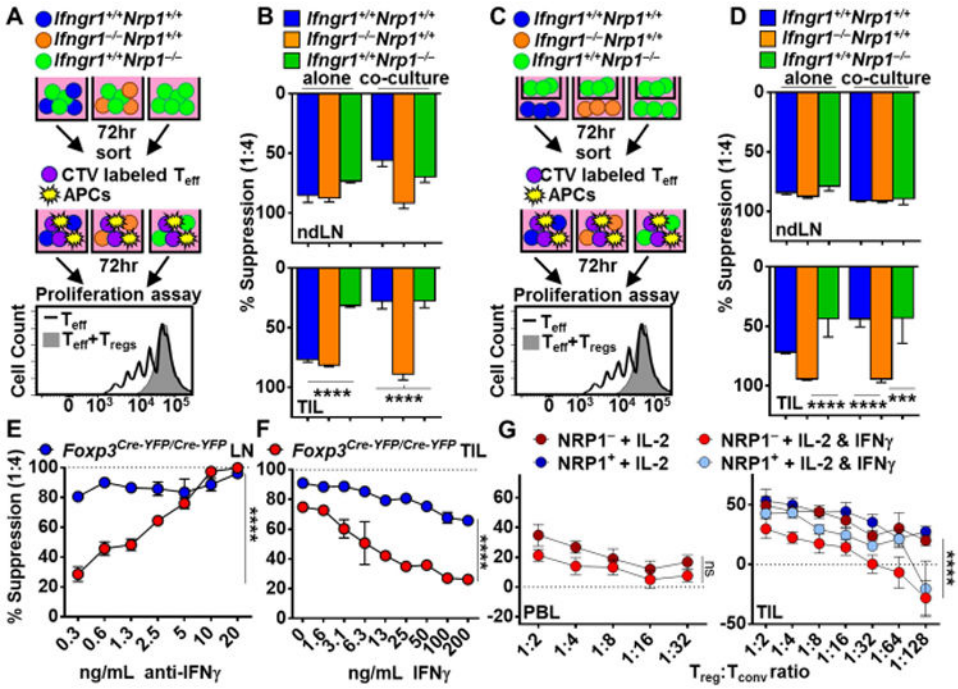

Figure 5. IFNγ reduces T_{reg} suppression

(**A, B**) T_{regs} were isolated from ndLN and TIL of mice noted, stimulated with PMA and Ionomycin, cultured with IL-2 alone or with IL-2 and *Nrp1*$^{-/-}$ T_{regs} for 72 hours and used in a microsuppression assay in absence of cytokine (n=6-7). (**C, D**) T_{regs} were isolated and stimulated as in (**A**), cultured in the bottom of a transwell plate with IL-2 alone or with IL-2 and *Nrp1*$^{-/-}$ T_{regs} in the top well for 72 hours and used in a microsuppression assay in the absence of cytokine (n=6-7). (**E**) T_{regs} were isolated from ndLN and TIL of *Foxp3*$^{Cre\text{-}YFP/Cre\text{-}YFP}$ mice, co-cultured with Nrp1$^{-/-}$ T_{regs} and IL-2 in the presence or absence of anti-IFNγ, re-sorted and used in a microsuppression assay in the absence of cytokine (n=6). (**F**) T_{regs} were isolated from ndLN and TIL of *Foxp3*$^{Cre\text{-}YFP/Cre\text{-}YFP}$ mice, treated with IL-2 and IFNγ for 72 hours, re-sorted and used in a microsuppression assay in the absence of cytokine (n=6). (**G**) T_{regs} were isolated from HNSCC PBL and TIL, cultured with IL-2 +/- IFNγ for 3 days, then used in a microsuppression assay in the absence of cytokine (n=2-14). Data represent 3-5 experiments. Error bars represent the mean ± SEM. Student unpaired t test (**A-D**) and 2 Way Anova (**E-G**) were used. (*p<0.05, **p <0.01, ****p <0.0001).

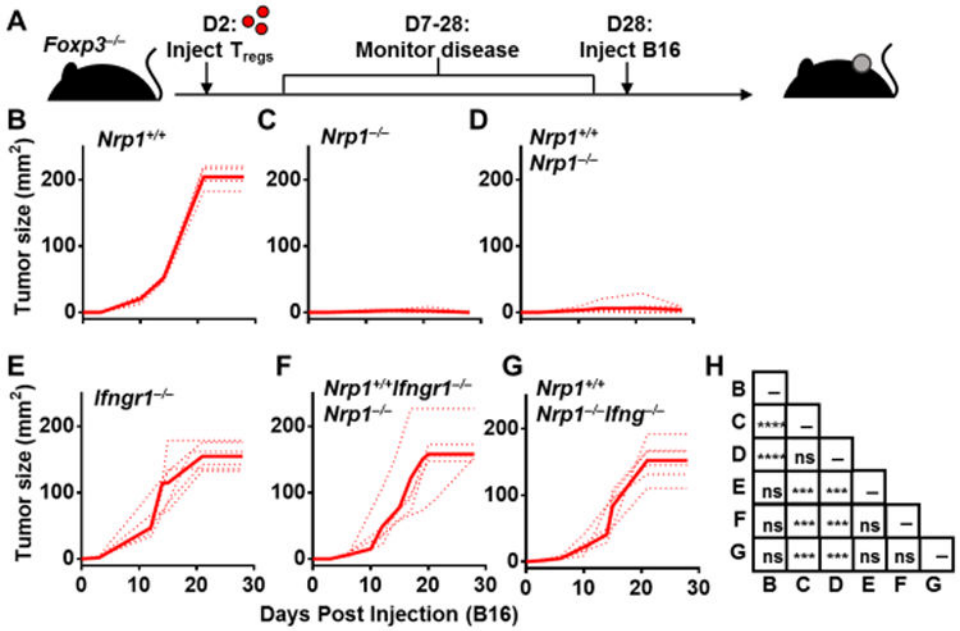

Figure 6. IFNγ uptake by T_{regs} is required for T_{reg} fragility and tumor clearance

(**A-G**) *Foxp3*$^{-/-}$ mice were injected with 10^6 T_{regs} on day 2 post-birth, and monitored for 28 days for the onset of any autoimmune symptoms [4 of 34 mice were removed from study], no more than 1 per experimental group. B16.F10 was injected ID on day 28 and tumor size was measured every 3 days. (**H**) Statistics of *Foxp3*$^{-/-}$ mice tumor growth. Data represent 5-7 independent experiments with 5-7 mice per experimental group. Error bars represent the mean ± SEM. 2 way ANOVA was used. (ns, not significant, ***$p < 0.001$, ****$p < 0.0001$).

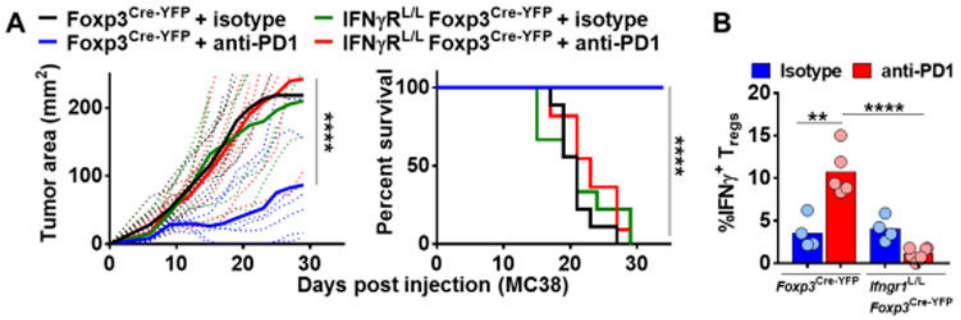

Figure 7. IFNγ-mediated T_{reg} fragility is required for antiPD1 response

(**A-B**) *Foxp3*$^{Cre\text{-}YFP}$ and *Ifngr1*$^{L/L}$*Foxp3*$^{Cre\text{-}YFP}$ mice were injected with MC38 SC on day 0 and treated with either anti-PD1 or isotype on days 6, 9, and 12 (200ug, 200ug, 200ug). (**A**) Tumor growth was measured with digital calipers every three days. Mice were removed from study when tumor growth reached a diameter of 2cm in any direction or when necrosis was observed, and survival plots were generated. (**B**) Lymphocytes were isolated from TIL on day 12 from *Foxp3*$^{Cre\text{-}YFP}$ and *Ifngr1*$^{L/L}$*Foxp3*$^{Cre\text{-}YFP}$ mice and were stimulated and stained for IFNγ. Data represent 2 independent experiments with 4-11 mice per experimental group. 2 way ANOVA (Fig. 7A), Kaplan-Meier test (Fig. 7A), and Student unpaired t test (Fig. 7B) were used (**p < 0.01, ***p<0.001, ****p < 0.0001).